

# Electromechanical Coupling Correction for Piezoelectric Layered Beams

E. B. Tadmor and Gábor Kósa

**Abstract**—This paper deals with the bending of layered piezoelectric beams (multimorphs) subjected to arbitrary electrical and mechanical loading. Weinberg [1] obtained a closed-form solution to this problem using Euler-Bernoulli beam theory and integrated equilibrium equations. In his analysis, Weinberg assumes that the electric field is constant through the thickness of the piezoelectric layers. This approximation is valid for materials with small electromechanical coupling (EMC) coefficients. In this paper, we relax this constraint and obtain a solution which accounts for the effect of strain on the electric field in the layers. We find that Weinberg’s solution can be extended to arbitrary EMC with a simple correction to the moment of inertia  $I$  of the piezoelectric layers. The EMC correction amounts to replacing  $I$  with  $(1 + \xi)I$ , where  $\xi$  is the square of the expedient coupling coefficient. The error in beam curvature introduced by neglecting the effect of EMC is shown to be proportional to  $\xi$ . This effect can be quite significant for modern piezoelectric materials which tend to have large EMC coefficients. The formulation is applied to three example cases: a cantilever unimorph, an asymmetric bimorph and a three-layer multimorph with an elastic core. The theoretical predictions for the last two examples are compared to simulations using the finite element method (FEM) and found to be in excellent agreement.

## I. INTRODUCTION

Piezoelectric layered beams often serve as sensors and actuators in microelectromechanical systems (MEMS) [2]. These structures, referred to as multimorphs, consist in general of thin layers of piezoelectric, dielectric, conductor and elastic materials. Multimorph devices operate in a bending mode resulting from the applied mechanical and electrical loading.

Weinberg [1] obtained a simple closed-form solution for the bending of piezoelectric multimorphs using Euler-Bernoulli beam theory, which neglects the effect of transverse shear on the deformation of the beam. The fundamental assumptions in this theory are that cross sections remain plane and normal to the deformed beam axis. These assumptions are appropriate given the slender geometry of typical multimorphs [3], [4]. In the solution, equilibrium is imposed in a weak sense using integrals over the the beam thickness. The resulting formulation is expressed in terms of effective cross section properties.

Weinberg’s analysis provides a clear and comprehensive modeling tool for the displacement and charge in a multimorph due to external moment, axial force and external electric field. However, one of the assumptions in the analysis is that the electric field in the piezoelectric layers is constant. This approximation is valid for materials with small electromechanical coupling (EMC) coefficients. Many piezoelectric materials satisfy

The authors are with the Department of Mechanical Engineering, Technion – Israel Institute of Technology, 32000 Haifa, Israel (email: tadmor@tx.technion.ac.il)

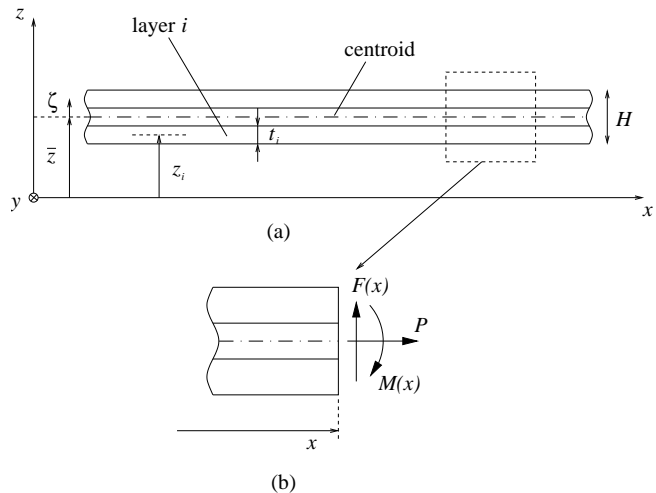


Fig. 1. Schematic diagram of (a) a portion of a multimorph beam, and (b) a section through the beam at position  $x$  showing the internal loads.

this condition, however modern piezoelectrics are designed to maximize the transfer of energy and thus tend to have large coupling coefficients [5].

In this paper we extend the Weinberg analysis to materials with arbitrary EMC coefficients by accounting for the variation of electric field in the beam layers. This variation is a result of EMC between the electric field and the non-uniform bending strain in the layers. Existing solutions which incorporate this effect have either been limited to the special case of bimorphs [6] or are significantly more complex than the Weinberg formulation [7]. We show that the Weinberg model [1] can be extended to materials with arbitrary EMC coefficients with a simple correction to the cross section inertia of the different layers. The fundamental difference between wide and narrow multimorphs is also discussed.

In the remainder of the paper, the term “EMC effect” refers to the effect of strain on the electric field in the piezoelectric layers due to EMC. The term “EMC correction” refers to the modification to the Weinberg model which accounts for this effect.

## II. LAYERED PIEZOELECTRIC BEAM MODEL

### A. Model Description and Assumptions

We consider a piezoelectric multimorph with  $m$  layers. The multimorph is loaded mechanically by application of distributed and point loads normal to the beam axis, and electrically by application of voltages across the piezoelectric layers. The mechanical loading results in a distribution of moment

$M(x)$  and shear force  $F(x)$  along the length of the beam. If the beam is prevented from extending in the axial direction, a constant axial force  $P$  may also be present. Fig. 1 shows a portion of the beam along with a section at position  $x$  showing the internal loads in their positive sense. The figure also shows the coordinate system (c.s.) and geometric parameters used in the analysis. The width of the beam is  $B$ .

The assumptions made in the derivation of the model are similar to those in [1]:

- 1) Each layer can be piezoelectric or purely elastic.
- 2) Each layer in the beam is in static equilibrium.
- 3) Displacements are continuous across the interfaces (i.e. no slip discontinuities exist at the interfaces).
- 4) Beam thickness is much less than the radius of curvature induced by the mechanical and electrical loading.
- 5) The cross section of the layers is constant along the length of the beam.

The additional assumption in [1] that EMC is small is relaxed here. Assumptions (3) and (4) together, allow the axial strain  $S$  at any point in the beam to be defined as

$$S(x, z) = -[z - z_N(x)]/R(x), \quad (1)$$

where  $z_N(x)$  and  $R(x)$  are the position of the neutral axis and radius of curvature, respectively, along the beam. Note that the neutral axis, which corresponds to the location of the unstrained fiber in the beam, is not equivalent to the centroid of the beam  $\bar{z}$ , unless the beam is loaded only by a moment distribution.

### B. Layer Constitutive Behavior

The linear three-dimensional piezoelectric constitutive relation at constant temperature is given in Voigt notation by [8]

$$S_m = s_{mn}^E T_n + d_{km} E_k, \quad (2)$$

where  $S_m$  and  $T_n$  are the strain and stress vectors, respectively,  $s_{mn}^E$  is the compliance matrix at constant electric field,  $d_{km}$  is the piezoelectric coupling matrix, and  $E_k$  is the electric field vector. The indices  $m$  and  $n$  run from 1 to 6, index  $k$  runs from 1 to 3, and the Einstein summation convention is assumed. For the one-dimensional (1D) beam problem we assume  $T_3 = 0$ . Two cases are considered for the out-of-plane stress: (1) plane stress conditions for narrow beams ( $B < 5H$ ), where  $T_2 = 0$ ; and (2) plane strain conditions for wide beams ( $B > 5H$ ), where  $S_2 = 0$ . The electric field is assumed to point in the  $z$ -direction, so that  $E_1 = E_2 = 0$ . In addition, we assume a material free of shear-tension coupling, such that  $s_{14}^E = s_{15}^E = s_{16}^E = 0$ . For now we focus on a generic layer in the multimorph without specifying the layer index. The material properties are assumed to be constant within each layer along the length of the beam. The mechanical and electrical fields, however, will vary along the  $x$  and  $z$  directions. No variation in the  $y$  direction is permitted due to the plane stress or strain condition applied. Given the above, relation (2) may be rewritten in 1D form as

$$T(x, z) = Y[S(x, z) - dE(x, z)], \quad (3)$$

where  $T = T_1$  and  $S = S_1$  are the axial stress and strain,  $E = E_3$  is the electric field in the  $z$ -direction, and  $Y$  and  $d$

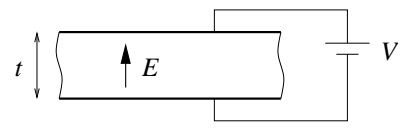


Fig. 2. The electric loading across a generic piezoelectric layer.

are the effective Young's modulus and piezoelectric coupling coefficient, respectively, given by

$$Y = \begin{cases} 1/s_{11}^E & \text{plane stress} \\ 1/\hat{s}_{11}^E = 1/(s_{11}^E - (s_{12}^E)^2/s_{22}^E) & \text{plane strain} \end{cases}, \quad (4)$$

$$d = \begin{cases} d_{31} & \text{plane stress} \\ \hat{d}_{31} = d_{31} - d_{32}s_{12}^E/s_{22}^E & \text{plane strain} \end{cases}. \quad (5)$$

It is now necessary to relate  $E(x, z)$  to the applied electric loading. Consider the case in Fig. 2, where a voltage  $V$  is applied across a piezoelectric layer of thickness  $t$ . If the layer were a simple dielectric, we would have,

$$E = -V/t. \quad (6)$$

For a piezoelectric layer, the effect of the variation of strain in the layer on the electric field in it must be accounted for. This effect was neglected in the Weinberg [1] formulation and is derived here.

Neglecting fringing effects, the electric displacement  $\mathbf{D}$  is constant in the layer at each point along the beam and is oriented along the  $z$ -direction.<sup>1</sup> The corresponding piezoelectric relation is

$$D_3 = d_{3m}T_m + \epsilon_{33}^T E_3, \quad (7)$$

where  $\epsilon_{33}^T$  is the dielectric constant. Subject to the same assumptions that led to the derivation of (3), we obtain the 1D form of (7),

$$E(x, z) = [D(x) - dT(x, z)]/\epsilon, \quad (8)$$

where the dependence on the coordinates has been made explicit,  $d$  is given by (5), and

$$\epsilon = \begin{cases} \epsilon_{33}^T & \text{plane stress} \\ \hat{\epsilon}_{33}^T = \epsilon_{33}^T - d_{32}^2/s_{22}^E & \text{plane strain} \end{cases}. \quad (9)$$

The voltage difference is constant along the beam and thus integrating (8) across the layer we have,

$$-V = \frac{1}{\epsilon} [tD(x) - d \int_{\text{layer}} T(x, z) dz]. \quad (10)$$

Defining  $\bar{T}$  as the average layer stress,

$$\bar{T}(x) = \frac{1}{t} \int_{\text{layer}} T(x, z) dz, \quad (11)$$

and rearranging (10) we have,

$$D(x) = d\bar{T}(x) - \epsilon V/t. \quad (12)$$

<sup>1</sup>This result is obtained from the differential form of Gauss's law  $\nabla \cdot \mathbf{D} = \rho$ , where  $\rho$  is the density of embedded charge in the layer. Assuming  $\rho = 0$  and that  $\mathbf{D} = D_3 \hat{\mathbf{k}}$ , this equation is simply  $\partial D_3 / \partial z = 0$  and thus  $D_3 = \text{const.}$

Substituting (12) into (8) gives

$$E(x, z) = -V/t - (d/\epsilon)[T(x, z) - \bar{T}(x)]. \quad (13)$$

Comparing (13) with (6), we see that EMC in the piezoelectric layer introduces a non-constant correction to the layer electric field. Next, we substitute the piezoelectric stress-strain relation (3) into (13), giving

$$E(x, z) = -V/t - (dY/\epsilon)[S(x, z) - \bar{S}(x) - d(E(x, z) - \bar{E}(x))], \quad (14)$$

where

$$\bar{S}(x) = \frac{1}{t} \int_{\text{layer}} S(x, z) dz, \quad (15)$$

$$\bar{E}(x) = \frac{1}{t} \int_{\text{layer}} E(x, z) dz. \quad (16)$$

Due to the geometry of the structure the average layer electric field  $\bar{E}$  is constant,

$$\bar{E}(x) = \bar{E} = -V/t. \quad (17)$$

This may be confirmed by substituting (13) into (16) and integrating. Substituting (17) into (14) and solving for  $E(x, z)$ , we have,

$$E(x, z) = -\frac{V}{t} - \frac{\xi}{d}[S(x, z) - \bar{S}(x)], \quad (18)$$

where  $\xi$  is the square of the expedient coupling coefficient  $k_e$  [6] defined as

$$\xi = k_e^2 = \frac{k^2}{1 - k^2}, \quad (19)$$

and  $k$  is the EMC coefficient defined by

$$k^2 = Y d^2 / \epsilon. \quad (20)$$

For plane stress,  $k^2 = d_{31}^2 / s_{11}^E \epsilon_{33}^T \equiv (k_{31}^l)^2$  where  $k_{31}^l$  is the EMC coefficient for axial stress only [8]. For plane strain,  $k^2 = \hat{d}_{31}^2 / \hat{s}_{11}^E \hat{\epsilon}_{33}^T \equiv (k_{31}^w)^2$  where  $k_{31}^w$  is the EMC coefficient for axial stress and plane strain conditions [8].

To this point our discussion has been general without specific mention of the layered structure of the multimorph beam or the strain relation for bending in (1) associated with it. To proceed further and obtain an explicit expression for  $E(x, z)$ , these factors must be introduced. We recall that the multimorph is comprised of  $m$  layers. Each layer  $i$  has effective material properties  $Y_i$ ,  $d_i$  and  $\epsilon_i$ , thickness  $t_i$ , and a voltage  $V_i$  across it. The location of the center of the layer is  $z_i$ , so that points inside layer  $i$  fall in the range  $z_i - t_i/2 < z < z_i + t_i/2$  (Fig. 1). In this notation the 1D piezoelectric relation in (3) for points in layer  $i$  becomes

$$T(x, z) = Y_i[S(x, z) - d_i E(x, z)]. \quad (21)$$

Next, we introduce the beam strain relation. Substituting (1) into (15), the average strain along layer  $i$  when subjected to bending is

$$\bar{S}_i(x) = -[z_i - z_N(x)]/R(x). \quad (22)$$

Substituting (1) and (22) into (18), we obtain the explicit form of  $E(x, z)$  in layer  $i$ ,

$$E(x, z) = -\frac{V_i}{t_i} + \frac{\xi_i}{d_i} \left( \frac{z - z_i}{R(x)} \right). \quad (23)$$

We may now combine the stress-strain relation in (21) with the electric field in (23) and the strain field in (1) to obtain the stress field within layer  $i$ ,

$$T(x, z) = Y_i \left[ -\frac{z - z_N(x)}{R(x)} - \xi_i \frac{z - z_i}{R(x)} + d_i \frac{V_i}{t_i} \right]. \quad (24)$$

If  $k_i^2 \ll 1$  then  $\xi_i \ll 1$  and the EMC term is negligible relative to the axial strain. In this case the constitutive relation reduces to (21) with a constant electric field  $-V_i/t_i$  as was used in [1].

### C. Application of Mechanical Equilibrium

The stress field in (24) contains the two unknown functions  $z_N(x)$  and  $R(x)$ . These functions may be obtained by imposing force and moment equilibrium on the beam. The condition for axial force equilibrium is,

$$\sum_i \int_{A_i} T(x, z) dA = P, \quad (25)$$

where  $A_i$  is the cross-sectional area of layer  $i$  ( $A_i = Bt_i$ ). Substituting in (24) and integrating gives

$$\frac{1}{R(x)} [\mathcal{F} z_N(x) - \mathcal{M}] - \mathcal{F}_E = P, \quad (26)$$

where

$$\mathcal{F} = \sum_i Y_i A_i, \quad (27)$$

$$\mathcal{F}_E = \sum_i Y_i A_i d_i \bar{E}_i, \quad \bar{E}_i = -V_i/t_i, \quad (28)$$

$$\mathcal{M} = \sum_i z_i Y_i A_i. \quad (29)$$

Constants  $\mathcal{F}$  and  $\mathcal{F}_E$  have units of force (N) and  $\mathcal{M}$  of moment (N·m). Note that the EMC term cancels out and relation (26) is identical to relation (6) in [1].

The condition for moment equilibrium is

$$\sum_i \int_{A_i} z T(x, z) dA = M(x). \quad (30)$$

Substituting in (24) and integrating gives

$$\frac{1}{R(x)} [\mathcal{K} - \mathcal{M} z_N(x)] + \mathcal{M}_E = -M(x), \quad (31)$$

where

$$\mathcal{M}_E = \sum_i z_i Y_i A_i d_i \bar{E}_i, \quad (32)$$

$$\mathcal{K} = \sum_i Y_i [(1 + \xi_i) I_i + A_i z_i^2]. \quad (33)$$

In (33),  $I_i = Bt_i^3/12$  is the moment of inertia of layer  $i$ . Constant  $\mathcal{M}_E$  has units of moment (N·m) and  $\mathcal{K}$  has units of N·m<sup>2</sup>.

Expression (31) is identical to relation (8) in Weinberg [1], except that  $I_i$  is multiplied by  $1 + \xi_i$ . This means that the effect of EMC on beam stiffness is to effectively increase the moment of inertia of each piezoelectric layer by  $1 + \xi_i = 1/(1 - k_i^2)$ . The solution now proceeds as in Weinberg [1]. Equations (26) and (31) may be solved together for the unknowns  $R(x)$  and  $z_N(x)$ ,

$$C(x) = \frac{(P + \mathcal{F}_E)\mathcal{M} - (M(x) + \mathcal{M}_E)\mathcal{F}}{\mathcal{F}\mathcal{K} - \mathcal{M}^2}, \quad (34)$$

$$z_N(x) = \frac{(P + \mathcal{F}_E)\mathcal{K} - (M(x) + \mathcal{M}_E)\mathcal{M}}{(P + \mathcal{F}_E)\mathcal{M} - (M(x) + \mathcal{M}_E)\mathcal{F}}, \quad (35)$$

where  $C(x) = 1/R(x)$  is the curvature.

The expressions in (34) and (35) may be simplified by setting the origin of the c.s. on the beam centroid. The location of the centroid  $\bar{z}$  is obtained from (35) by setting  $P = 0$  and  $E_i = 0$  (i.e. pure moment loading),

$$\bar{z} = \frac{\sum_i z_i Y_i A_i}{\sum_i Y_i A_i} = \frac{\mathcal{M}}{\mathcal{F}}. \quad (36)$$

We define  $\zeta = z - \bar{z}$  as the new coordinate in the  $z$ -direction with origin at  $\bar{z}$  (Fig. 1). In the new c.s., the parameters  $\mathcal{M}$ ,  $\mathcal{M}_E$  and  $\mathcal{K}$  are recomputed as  $\hat{\mathcal{M}}$ ,  $\hat{\mathcal{M}}_E$  and  $\hat{\mathcal{K}}$  using the same definitions as before with  $z_i$  replaced by  $\zeta_i$ . The advantage of this is that since  $\bar{\zeta} = 0$ , then from (36) we have  $\hat{\mathcal{M}} = 0$ . Relations (34) and (35) are then,

$$C(x) = -\frac{M(x) + \hat{\mathcal{M}}_E}{\hat{\mathcal{K}}}, \quad (37)$$

$$\zeta_N(x) = -\frac{(P + \mathcal{F}_E)\hat{\mathcal{K}}}{(M(x) + \hat{\mathcal{M}}_E)\mathcal{F}}. \quad (38)$$

It is of interest to evaluate the error in curvature introduced by neglecting the EMC effect in order to quantify its importance. If the EMC effect is neglected, the resulting error in curvature is

$$\text{err} = \frac{C(x)|_{\xi=0} - C(x)}{C(x)} = \frac{\sum_{i \in \text{piezo}} Y_i I_i \xi_i}{\sum_i Y_i [I_i + A_i \zeta_i^2]} = \sum_{i \in \text{piezo}} B_i \xi_i. \quad (39)$$

In (39),  $\sum_{i \in \text{piezo}}$  indicates summation only over piezoelectric layers. The total error is thus a linear function of the coupling coefficients of the piezoelectric layers. For systems where all piezoelectric layers are composed of the same material with coupling coefficient  $\xi$ , the error will be proportional to this value,

$$\text{err} = \left[ \frac{\sum_{j \in \text{piezo}} Y_j I_j}{\sum_i Y_i [I_i + A_i \zeta_i^2]} \right] \xi. \quad (40)$$

The maximum possible error in curvature in this case is  $\xi$ , which is obtained for a piezoelectric unimorph composed of a single piezoelectric layer with electrodes of negligible thickness. For this case,  $\sum_i A_i \zeta_i^2 = 0$ , and the sums in the numerator and denominator cancel out. For multimorphs, the maximum error is approached in structures where one of the piezoelectric layers is significantly thicker than all other layers combined, so that  $\sum_i A_i \zeta_i^2$  is small.

Modern piezoelectric materials for actuator applications are designed to have large piezoelectric coefficients  $d_{ij}$  in order to

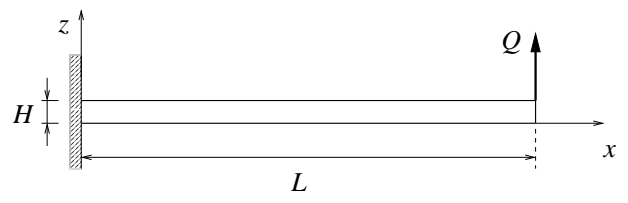


Fig. 3. Schematic of the cantilever unimorph example.

maximize the transfer of electrical energy to mechanical energy [5]. A consequence of this is that piezoelectric actuator materials have large EMC coefficients. The effect is accentuated under plane strain conditions. For PZT-5A, for example,  $\xi = 0.136$  under plane stress conditions and  $\xi = 0.391$  under plane strain conditions. This means that the maximum error in curvature for this material can reach nearly 40% for plane strain structures. This is a substantial effect.

#### D. Governing Equations

The curvature  $C(x)$  along the length of the beam is given in (37). The deflection of the beam in the  $z$ -direction  $w(x)$  may be obtained from this relation, by noting that for small displacements  $C(x) \approx d^2w/dx^2$ , so that

$$\hat{\mathcal{K}} \frac{d^2w}{dx^2} = -M(x) - \hat{\mathcal{M}}_E. \quad (41)$$

In the absence of axial constraints (i.e.  $P = 0$ ), the solution is straightforward and may be obtained from (41) by integration and application of boundary conditions. For the axially constrained case, the moment generated by the axial force due to its vertical displacement must be accounted for. The resulting beam-column equation is

$$\hat{\mathcal{K}} \frac{d^4w}{dx^4} - P \frac{d^2w}{dx^2} = q(x), \quad (42)$$

where  $q(x)$  is the external distributed load per unit length acting normal to the beam axis. This equation must be solved subject to the displacement boundary conditions and the curvature relation in (41).

Lumped model solutions to equations (41) and (42) for a cantilever and a built-in multimorph are given in Weinberg [1]. The EMC correction to these solutions simply involves replacing the moments of inertia  $I_i$  with effective moments of inertia  $\bar{I}_i = (1 + \xi_i)I_i$ .

### III. REPRESENTATIVE EXAMPLES

In this section we present three examples that demonstrate the influence of the EMC correction. In the examples, the predictions of the current model with the EMC effect included (“corrected model”) are compared with the Weinberg [1] model (“standard model”).

#### A. Cantilever Unimorph

The first example considered is a single-layered piezoelectric cantilever beam of length  $L$  and cross section dimensions  $B$  and  $H$  (Fig. 3). The beam is loaded by a concentrated force  $Q$  at its

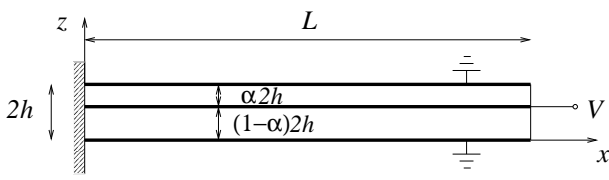


Fig. 4. Schematic of the asymmetric bimorph example. The thick black lines represent electrodes that are neglected in the analysis.

end. No electrical loading is applied. The curvature along the beam is obtained from (37) by setting  $\hat{\mathcal{M}}_E = 0$ ,

$$C(x) = -M(x)/\hat{\mathcal{K}}. \quad (43)$$

The moment distribution in the beam is  $M(x) = -Q(L - x)$  and  $\hat{\mathcal{K}} = (1 + \xi)IY$ , where  $\xi$  and  $Y$  are the beam material properties and  $I = BH^3/12$ . The curvature is then

$$C(x) = Q(L - x)/(1 + \xi)IY. \quad (44)$$

Integrating this relation, the beam deflection function is

$$w(x) = \frac{1}{6}QL^3 \left[ \left(1 - \frac{x}{L}\right)^3 + 3\frac{x}{L} - 1 \right] / (1 + \xi)IY. \quad (45)$$

The deflection at the end of the beam is  $\delta \equiv w(L) = QL^3/3(1 + \xi)IY$ . The error in the end deflection, when neglecting the EMC effect, is  $(\delta|_{\xi=0} - \delta)/\delta = \xi$ . Thus for a piezoelectric unimorph used as a sensor, such as an AFM beam [2], neglecting the EMC effect can result in large errors.

### B. Asymmetric Bimorph

The second example we present is an asymmetric bimorph (Fig. 4). The bimorph has a fixed height  $H = 2h$  and layers of different thickness  $(1 - \alpha)2h$  and  $\alpha 2h$ , where  $\alpha$  is a parameter ranging from 0 to 1. The structure is built-in at one end and loaded electrically by short-circuiting the top and bottom surfaces and applying a voltage  $V$  at the interface between the two layers. Both layers are composed of the same piezoelectric material with the same crystallographic orientation. The stiffness of the electrode layers is neglected.

The curvature of the bimorph due to the applied electrical loading is constant along the  $x$ -axis and is obtained from (37) by setting  $M(x) = 0$ ,

$$C_E = -\hat{\mathcal{M}}_E/\hat{\mathcal{K}}. \quad (46)$$

The centroid of the bimorph is located at  $\bar{z} = h$ . Given this, the parameters  $\hat{\mathcal{M}}_E$  and  $\hat{\mathcal{K}}$  in (46) can be shown to be,

$$\hat{\mathcal{M}}_E = YBhdV, \quad (47)$$

$$\hat{\mathcal{K}} = (2/3)YBh^3[1 + \xi(3\alpha^2 - 3\alpha + 1)], \quad (48)$$

and thus

$$C_E = -\frac{3dV}{2h^2[1 + \xi(3\alpha^2 - 3\alpha + 1)]}. \quad (49)$$

If the EMC effect is neglected ( $\xi = 0$ ), the predicted curvature is independent of  $\alpha$ ,

$$C_E(\xi = 0) = -3dV/2h^2. \quad (50)$$

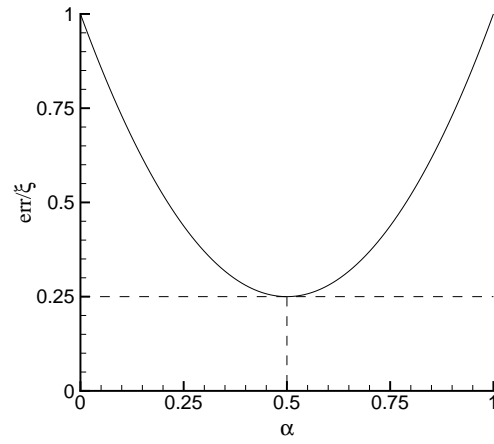


Fig. 5. Error incurred by neglecting the EMC effect in an asymmetric bimorph.

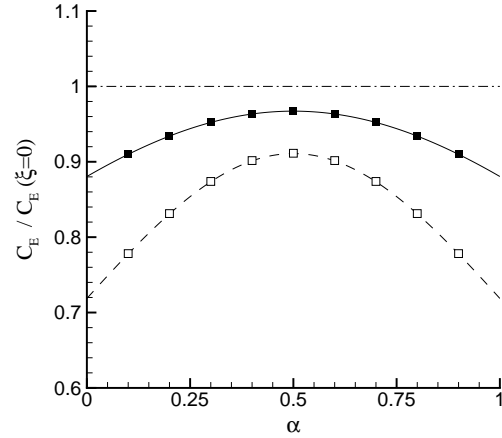


Fig. 6. Comparison between theory and FEM simulations for the curvature of the asymmetric bimorph. The curvature is normalized by the curvature predicted by the standard model. The lines correspond to the predictions of the theory and the symbols to the FEM results. Plane stress results are the solid line and filled symbols. Plane strain results are the dashed line and hollow symbols. The dash-dot line corresponds to the prediction of the standard theory.

The error in curvature introduced by neglecting the EMC effect is

$$\text{err} = \frac{C_E(\xi = 0) - C_E}{C_E} = \xi(3\alpha^2 - 3\alpha + 1). \quad (51)$$

The error scales with  $\xi$  and increases the more asymmetric the beam becomes (Fig. 5). The error is maximum at  $\alpha = 0$  and  $\alpha = 1$  where it reaches  $\xi/2$ . For a symmetric bimorph ( $\alpha = 0.5$ ) the error is  $\xi/4$ .

To verify the model, FEM calculations were carried out using the commercial package ANSYS for a bimorph with dimensions  $2h = 10 \mu\text{m}$  and  $L = 500 \mu\text{m}$ , and applied voltage  $V = 1 \text{ V}$ . The layers are composed of PZT-5A with material parameters given in Table I. The poling axis of the piezoelec-

<sup>2</sup>The results at  $\alpha = 0$  and  $\alpha = 1$  are, of course, non-physical since at these points the bimorph becomes single-layered and no curvature is expected. As  $\alpha \rightarrow 0$  or  $\alpha \rightarrow 1$  the behavior of the system is expected to deviate from the theory as the electrodes across the infinitesimally thin layer interact and eventually short-circuit.

		PZT-5A	Pt{111}
Relative Permittivity	$\epsilon_{33}^T/\epsilon_0$	1700	–
Compliance (TPa <sup>-1</sup> )	$s_{11}^E = s_{22}^E$	16.3	5.40
	$s_{12}^E$	-5.67	-2.43
Piezoelectric (pC/N)	$d_{31} = d_{32}$	-171	–

TABLE I

MATERIAL PARAMETERS FOR PZT-5A TAKEN FROM [9] AND Pt WITH {111} TEXTURE COMPUTED USING THE FORMULATION IN [10] WITH SINGLE CRYSTAL CONSTANTS FROM [11].

	plane stress	plane strain
$Y$ [GPa]	61.52	70.05
$d$ [pC/N]	-171.0	-230.7
$\epsilon$ [nF/N]	15.05	13.25
$k$	0.346	0.530
$\xi$	0.136	0.391

TABLE II

EFFECTIVE 1D MATERIAL CONSTANTS AND ASSOCIATED EMC COEFFICIENTS FOR PZT-5A WITH POLING ORIENTED ALONG THE MULTIMORPH  $z$ -AXIS FOR BOTH PLANE STRESS AND PLANE STRAIN CONDITIONS.

tric layers is aligned with the bimorph  $z$ -axis. The effective 1D material constants and EMC coefficients are given in Table II. The simulations were carried out for both plane stress and plane strain conditions using the two-dimensional, 4-noded, coupled-field solid element PLANE13. A uniform mesh was used with 200 elements along the length of the beam and 30 elements in the thickness direction for a total of 6000 elements. The results for the two cases are presented in Figs. 6. The simulation results appear as square symbols and the theoretical predictions as the lines. The agreement between model and simulation for both plane stress and plane strain is excellent. The dash-dot line in the figure is the result predicted by the standard model [1]. For plane stress, the standard model predicts a curvature of  $C_E(\xi = 0) = 10.26 \text{ m}^{-1}$ . This result deviates from the actual curvature, obtained in the simulation and predicted by the corrected theory, by 3.4% for the symmetric bimorph ( $\alpha=0.5$ ) and by 9.9% for the most asymmetric cases tested ( $\alpha=0.1$  and  $\alpha=0.9$ ). For plane strain, the prediction of the standard model for the curvature is  $C_E(\xi = 0) = 13.84 \text{ m}^{-1}$  and the observed deviations are 9.8% for the symmetric case and 28.6% for the asymmetric end cases. For a real beam with finite width, the results are expected to fall somewhere within the range set by the plane stress and plane strain results. Although in this case the effect of anticlassic curvature must also be considered [12].

### C. Symmetric Three-Layer Multimorph

The final example considered is a symmetric three-layer multimorph with piezoelectric layers on the outside and a central

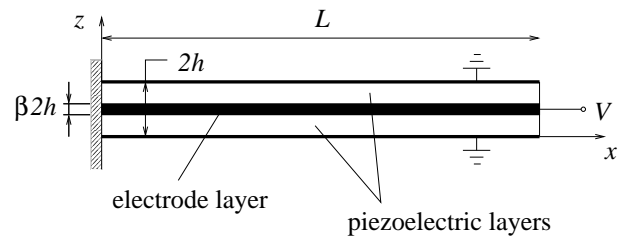


Fig. 7. Schematic of the symmetric three-layer multimorph example.

electrode of finite thickness which plays an elastic role in addition to its electrical function (Fig. 7). This design corresponds to the parallel bimorph structure defined in [13]. The multimorph has fixed height  $H = 2h$ . The thickness of the central electrode is  $\beta 2h$  where  $\beta$  can vary from 0 to 1. With  $\beta = 0$ , the bimorph of the previous section is recovered for the case  $\alpha = 0.5$ . The influence of the outer electrodes is neglected. The electric boundary conditions are the same as those defined in the previous section, with the central electrode set to a voltage  $V$  and the outer electrodes shorted. As before, the piezoelectric layers are taken to be symmetric in the  $x$ - $y$  plane so that the poling axis is aligned with the multimorph  $z$ -direction. The parallel bimorph structure was selected for this example in order to reduce the complexity of the resulting expressions. The effect of EMC is not very large for this case. In order to emphasize it we focus on the plane strain case where the effect is more pronounced. In practical applications, parallel bimorphs are less common than unimorph designs where the EMC effect is larger.

The curvature of the multimorph due to the applied electrical loading is given by (46). The centroid of the multimorph is located at  $\bar{z} = h$ , and with this, the parameters  $\hat{\mathcal{M}}$  and  $\hat{\mathcal{K}}$  can be shown to be,

$$\hat{\mathcal{M}}_E = (1 + \beta)YBhdV, \quad (52)$$

$$\hat{\mathcal{K}} = \frac{YBh^3}{6} [(1 - \beta)[(1 + \xi)(1 - \beta)^2 + 3(1 + \beta)^2] + 4\eta\beta^3], \quad (53)$$

where the material constants  $Y$ ,  $d$  and  $\xi$  are those of the piezoelectric layers, and  $\eta = Y_e/Y$ , where  $Y_e$  is the effective Young's modulus of the electrode layer. Substituting (52) and (53) into (46), the multimorph curvature is given by,

$$C_E = -\frac{6(1 + \beta)dV}{h^2 [(1 - \beta)[(1 + \xi)(1 - \beta)^2 + 3(1 + \beta)^2] + 4\eta\beta^3}. \quad (54)$$

If the EMC effect is neglected the curvature is

$$C_E(\xi = 0) = -\frac{3(1 + \beta)dV}{2h^2 [1 + (\eta - 1)\beta^3]}. \quad (55)$$

Note that in this case, the standard theory result is not independent of the geometry as it was in the previous example. For  $\beta=0$ , the result in (50) is recovered. For  $\beta=1$ ,  $C_E(\xi = 0) = -3dV/\eta h^2$ . At this limit the electrode occupies the entire thickness of the multimorph. The result in this case is non-physical for the same reasons given earlier.

To verify the model, FEM calculations were carried out using the same methodology detailed in the previous section. The

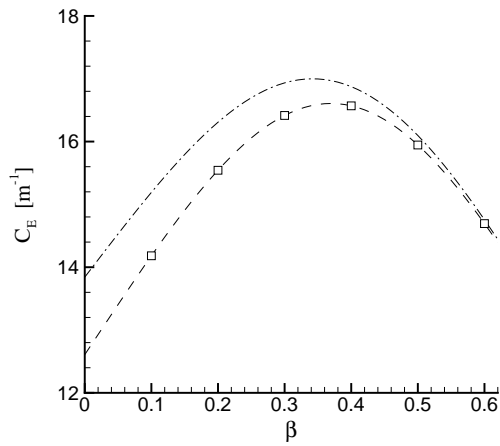


Fig. 8. Comparison between theory and FEM simulations for the curvature of the symmetric three-layer multimorph under plane strain conditions. The lines correspond to the predictions of the theoretical models: standard (dash-dot) and corrected (dashed). The symbols are the results of FEM simulations.

piezoelectric layers were taken to be of PZT-5A and the central electrode of Pt with  $\{111\}$  texture in the  $z$ -direction. Both common choices for piezoelectric multimorphs [2]. The material properties are given in Table I. The elastic constants of the textured Pt were calculated using the formulation in [10] with single crystal constants from [11]. The effective 1D constants for the piezoelectric layers are given in Table II. The effective Young's modulus of the Pt layer under plane strain conditions is  $Y_e = 232.5$  GPa, so  $\eta = 3.32$ . The remaining parameters are the same as those used in the previous section ( $2h = 10$   $\mu\text{m}$ ,  $L = 500$   $\mu\text{m}$ ,  $V = 1$  V). Fig. 8 shows the curvature as a function of  $\beta$ , predicted by the standard model (dash-dot line) and the corrected theory (dashed line), along with the FEM results (hollow squares). The FEM results are in excellent agreement with the corrected theory. The maximum deviation between the standard and corrected models occurs at  $\beta = 0$ . As  $\beta \rightarrow 1$ , the standard and corrected theories coincide.

#### IV. CONCLUSIONS

A general theory is derived for layered piezoelectric beams which accounts for the variation of electric field in the beam layers due to EMC between the strain and electric field. The theory is an extension of the formulation in Weinberg [1] which neglects this effect. It is found that the EMC correction to Weinberg's formulation is achieved simply by replacing the moment of inertia of the piezoelectric layers  $I$  with an effective moment of inertia  $\bar{I} = (1 + \xi)I$  where  $\xi$  is the square of the expedient coupling coefficient [6]. With this substitution made, all results in [1] remain valid, including the expressions for piezoelectric sensing and the lumped parameter models. The error introduced to the beam curvature by neglecting the EMC effect is a linear function of the coupling coefficients of the piezoelectric layers,

$$\text{err} = \sum_{j \in \text{piezo}} B_j \xi_j. \quad (56)$$

The proportionality factors  $B_j$  in (56) are functions of the layer geometry and effective Young's modulus. For a beam contain-

ing a single piezoelectric layer with coupling coefficient  $\xi$ , or one where all piezoelectric layers are composed of the same material, the error is proportional to  $\xi$ . The magnitude of the error increases for multimorphs where one of the piezoelectric layers is significantly thicker than all other layers combined. The maximum possible error is  $\xi$  which is obtained for a piezoelectric unimorph. For PZT-5A for example  $\xi = 0.136$  for plane stress conditions and  $\xi = 0.391$  for plane strain conditions, so the effect can be substantial.

Three different examples were presented to demonstrate the EMC effect. The first example was a cantilever unimorph loaded by a concentrated force at its end. The error in tip deflection introduced by neglecting the EMC effect is equal to  $\xi$ . The second example was an asymmetric bimorph with layers of thickness  $\alpha 2h$  and  $(1 - \alpha)2h$  loaded electrically by a voltage applied between the piezoelectric layers. If the EMC effect is neglected, the predicted curvature is independent of the asymmetry parameter  $\alpha$ . With the effect included, the curvature is an inverse quadratic function of  $\alpha$ . The maximum error is  $\xi$ . The final example, is a symmetric three-layer multimorph with an elastic core, loaded electrically as in the previous example. The second and third examples were verified by FEM calculations for PZT-5A piezoelectric layers and Pt electrodes with  $\{111\}$  texture. Both plane stress and plane strain conditions were tested. The agreement between theory and simulation were excellent in both cases.

#### ACKNOWLEDGMENT

The authors gratefully acknowledge the contribution of Yogev Or for carrying out the finite element calculations.

#### REFERENCES

- [1] M. S. Weinberg, "Working equations for piezoelectric actuators and sensors", *J. Microelectromech. Syst.*, vol. 8, pp. 529–533, Dec. 1999.
- [2] P. Muralt, "Ferroelectric thin films for micro-sensors and actuators: a review", *J. Micromech. Microeng.*, vol. 10, pp. 136–146, June 2000.
- [3] I. Kanno, "Piezoelectric properties of c-axis oriented  $\text{Pb}(\text{Zr,Ti})\text{O}_3$  thin films", *Appl. Phys. Lett.*, vol. 70, pp. 890–896, April 1997.
- [4] J. Akedo, and M. Lebedev, "Piezoelectric properties and poling effect of  $\text{Pb}(\text{Zr,Ti})\text{O}_3$  thick films prepared for microactuators by aerosol deposition", *Appl. Phys. Lett.*, vol. 77, pp. 1710–1712, Nov. 2000.
- [5] S. E. Park, and T. R. Shrout, "Ultrahigh strain and piezoelectric behavior in relaxor based ferroelectric single crystals", *J. Appl. Phys.*, vol. 82, pp. 1804–1811, August 1997.
- [6] T. Ikeda, *Fundamentals of Piezoelectricity*. Oxford, 1996.
- [7] M. Krommer, and H. Irschik, "An electromechanically coupled theory for piezoelectric beams taking into account the charge equation of electrostatics", *Acta Mech.*, vol. 154, pp. 141–158, 2002.
- [8] IEEE Std 176-1987, Standard on Piezoelectricity.
- [9] R. Bechmann, and R. F. S. Hearmon, *Elastic, Piezoelectric, Piezooptic and Electrooptic Constants of Crystals*. Springer, 1966.
- [10] D. Baral, J. E. Hilliard, J. B. Ketterson, and K. Miyano, "Determination of the primary elastic constants from thin foils having a strong texture", *J. Appl. Phys.*, vol. 53, pp. 3552–3559, May 1982.
- [11] G. Simmons, and H. Wang, *Single Crystal Elastic Constants and Calculated Aggregate Properties*. MIT Press, 1971.
- [12] S. Senturia, *Microsystem Design*. Kluwer, 2000.
- [13] J. G. Smits, S. I. Dalke, and T. K. Cooney, "The constituent equations of piezoelectric bimorphs", *Sensors and Actuators A*, vol. 28, pp. 41–61, Sept. 1991.



**Ellad B. Tadmor** received the B.Sc. and M.Sc. degrees in mechanical engineering from the Technion – Israel Institute of Technology in Haifa, Israel, and the Ph.D. degree in solid mechanics from Brown University in Providence, RI. He was a postdoctoral research fellow at the Division of Engineering and Applied Science, Harvard University, Cambridge, MA. He is currently a senior lecturer in the Department of Mechanical Engineering at the Technion. His research focuses on understanding material response from fundamental principles rather than phenomenology.

He studies microscopic processes that lead to macroscopic phenomena such as fracture and plasticity using atomic-scale modeling and multiple-scale techniques. His interest in MEMS focuses on the response of piezoelectric materials and on the mechanical failure of MEMS devices.



**Gábor Kósa** was born in Romania in 1972. He immigrated to Israel in 1982, received his B.Sc. degree *cum laude* in mechanical engineering from the Technion – Israel Institute of Technology in Haifa in 1995. From 1995 to 1998 he served in the Israel Defense Force (IDF) as a research engineer. In 2001 he received his M.Sc. degree from the Technion. He was employed in RAFAEL, the Armament Development Authority, in Haifa from 2000 to 2001 as a research and development engineer of microelectromechanical systems. Currently he is doing his Ph.D. in the

field of medical micro-robots in the Technion. His research interests include modeling of microsystems and robotics.